Graphene Oxide as an Ideal Substrate for Hydrogen Storage

Lu Wang,[†,‡] Kyuho Lee,[‡] Yi-Yang Sun,[‡] Michael Lucking,[‡] Zhongfang Chen,[§] Ji Jun Zhao,[†] and Shengbai B. Zhang[‡,*]

[†]Laboratory of Materials Modification by Laser, Electron, and Ion Beams, School of Physics and Optoelectronic Technology and College of Advanced Science and Technology, Dalian University of Technology, Dalian 116024, China, [‡]Department of Physics, Applied Physics, and Astronomy, Rensselaer Polytechnic Institute, Troy, New York 12180, and [§]Department of Chemistry, Institute for Functional Nanomaterials, University of Puerto Rico, San Juan, Puerto Rico 00931

ABSTRACT Organometallic nanomaterials hold the promise for molecular hydrogen (H_2) storage by providing nearly ideal binding strength to H_2 for room-temperature applications. Synthesizing such materials, however, faces severe setbacks due to the problem of metal clustering. Inspired by a recent experimental breakthrough (*J. Am. Chem. Soc.* 2008, *130*, 6992), which demonstrates enhanced H_2 binding in Ti-grafted mesoporous silica, we propose combining the graphene oxide (GO) technique with Ti anchoring to overcome the current synthesis bottleneck for practical storage materials. Similar to silica, GO contains ample hydroxyl groups, which are the active sites for anchoring Ti atoms. GO can be routinely synthesized and is much lighter than silica. Hence, higher gravimetric storage capacity can be readily achieved. Our first-principles computations suggest that GO is primarily made of low-energy oxygen-containing structural motifs on the graphene sheet. The Ti atoms bind strongly to the oxygen sites with binding energies as high as 450 kJ/mol. This is comparable to that of silica and is indeed enough to prevent the Ti atoms from clustering. Each Ti can bind multiple H_2 with the desired binding energies (14−41 kJ/mol-H_2). The estimated theoretical gravimetric and volumetric densities are 4.9 wt % and 64 g/L, respectively.

KEYWORDS: graphene oxide · titanium anchoring · hydrogenation · hydrogen storage · first-principles computations

Molecular hydrogen (H_2) sorbents are appealing materials for storing hydrogen fuel onboard vehicles. The uptake and release of H_2 fuel in the sorbent materials can be fast and require less heat transfer. To use the H_2 sorbents at near ambient conditions, the binding energy of H_2 in these materials must be within certain range (*e.g.*, 20−40 kJ/mol).[1,2] Theoretical studies predicted[3,4] that Kubas-like interactions between transition metal (TM) centers and coordinated H_2 could fall within this desirable energy range. Such predictions are consistent with recent experimental studies by using metal−organic frameworks (MOFs) with under-coordinated TM.[5−8] Attempts to anchor TM directly on carbon nanostructures, however, have not yet been successful. Recently, Hamaed *et al.* used organometallic precursor to successfully graft Ti onto the inner surface of mesoporous silica.[9] Though this work demonstrated the feasibility of individually dispersing Ti and the capability of binding multi-H_2 by dispersed Ti, mesoporous silica has a relatively small surface-to-volume ratio and may be too heavy for practical hydrogen storage.

So far, no practical H_2 sorbent is available. Finding the right material for onboard storage is still a grand challenge. Concerning TM-based organometallic sorbents, several conditions are required at the same time: First, the substrate materials possess high surface-to-volume ratio and are lightweight. Second, the TM atoms are under-coordinated and well-exposed to accommodate multi-H_2. Third, these unsaturated TM atoms, despite their high chemical reactivity,[10] do not form clusters. These require that the anchoring bonds between the TM atoms and the substrate are strong and the TM coverage is also optimized. Along the line of strengthening the anchoring bonds, several strategies have been suggested, such as functionalizing organic molecules,[11] employing defect sites in carbon materials,[12,13] and directly integrating metal atoms into the skeleton.[14,15]

Alternatively, graphene oxide (GO) can be a potential substrate to covalently anchor TM atoms by simultaneously satisfying all these three conditions. GO has large surface-to-volume ratio and is intrinsically lightweight (condition 1). GO possesses ample O sites on the surfaces. Oxygen is the key in anchoring under-coordinated Ti (condition 2) and enhancing the TM−substrate binding (condition 3), as having been experimentally demonstrated on mesoporous silica.[9]

Although GO has been routinely synthesized and extensively studied,[16−24] currently its precise atomic structures are still under intense investigation. In fact, the O content of GO can vary greatly, depending

*Address correspondence to zhangs9@rpi.edu.

Received for review June 24, 2009 and accepted September 16, 2009.

Published online September 22, 2009.
10.1021/nn900667s CCC: $40.75

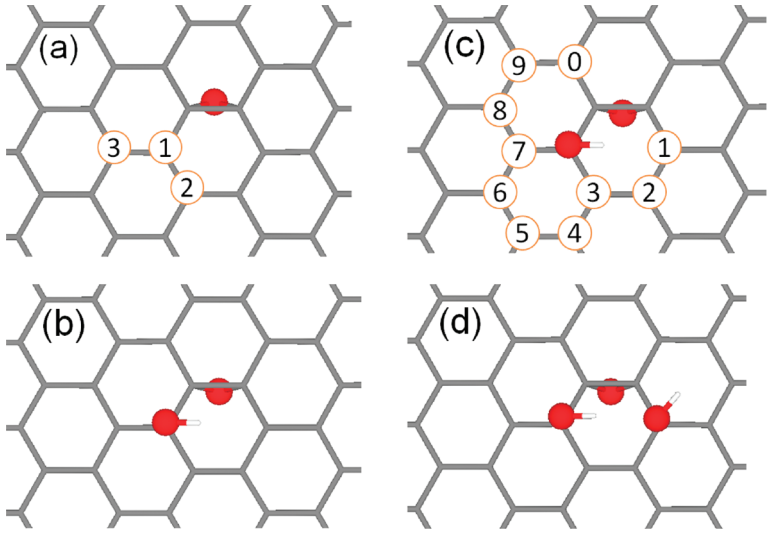

Figure 1. (a) Possible positions to form an (−O−, −OH) pair, (b) the most stable (−O−, −OH) pair, (c) possible positions to form an (−O−, 2−OH) complex starting from (b), and (d) one of the most stable (−O−, 2−OH) motifs, which is used throughout the paper.

on the experimental conditions in which H usually coexists. Under the O-rich conditions, GO contains epoxy, whereas under the H-rich conditions, hydrogenated graphene will form. In the intermediate region, GO usually contains both epoxies (−O−) and hydroxyls (−OH).

In this paper, we report first-principles studies of GO with comparable −O−, −OH, and sp^2 carbon (C) ratios. We identify a basic structural motif that consists of one −O− and two −OH as the basic building blocks of low-energy GO for such compositions. We investigate how to securely anchor Ti on GO without having to compromise the required exposure of metal to H_2. The calculated Ti−O binding energies are, in fact, comparable to those on mesoporous silica, suggesting that Ti clustering is no longer a problem. We then calculate the binding energies of H_2 to Ti. Despite the significantly enhanced metal−substrate binding *via* the O, the anchored Ti atoms are still able to bind multi-H_2 with suitable energies for room-temperature storage. The theoretical gravimetric and volumetric densities are 4.9 wt % and 64 g/L, respectively.

RESULTS AND DISCUSSION

Structural Models. As mentioned before, GO structural model from experiment is not available. Recently, Cai and co-workers investigated the structure of GO by solid-state NMR experiments.[25] They found that −O− and −OH are the two dominant O groups on the surface by clearly distinguishing three types of C atoms, namely, the sp^2 carbon and two types of sp^3 carbon bonded to hydroxyls and epoxies, respectively. The concentrations of these three types of carbon are comparable, suggesting that the C(sp^2)/C(−O−)/C(−OH) ratio of 1:1:1 is representative of the GO. Moreover, it suggests that the two types of O groups are in proximity, possibly as nearest neighbors.

Using a large 10 × 10 supercell, we have performed a comprehensive search for the most stable local structural motifs consisting of −O− and −OH. First, we put an −O− at the center of the supercell and then place an −OH at the three inequivalent nearby carbon sites shown in Figure 1a. The lowest-energy motif is the one where the −O− and −OH are the nearest neighbors but located at the opposite sides of the graphene sheet, as shown in Figure 1b. In general, the (−O−, −OH) pairs are high-energy motifs because the creation of a dangling bond (DB) by the attachment of a single −OH. To stabilize them, we can add another −OH to the labeled sites in Figure 1c to form an (−O−, 2−OH) motif. There are two such configurations with low energy, labeled as site 1 and site 3.

There are four major factors that need to be considered for optimal stability: (i) the accommodation of hydrogen bonding within an (−OH, −OH) pair or an (−OH, −O−) pair, (ii) the reduction of strain and Coulomb repulsion among negatively charged oxygen ions, (iii) the elimination of DB, and (iv) the proximity of −OH to −O−. In Figure 1c, the second −OH at site 3 or site 7 is on the opposite side of the graphene sheet with respect to the first −OH and forms a hydrogen bond with the −O− on the same side; the second −OH at the other sites is on the same side of the first −OH and forms a hydrogen bond with the first −OH. This is corresponding to condition (i). Taking the structure in Figure 1d as an example, we find that hydrogen bond-

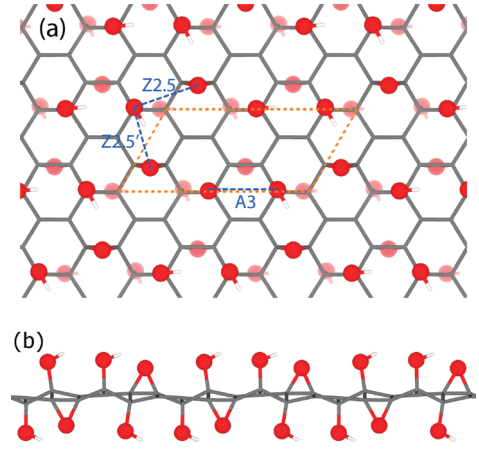

Figure 2. GO model constructed by spatially repeating the motif in Figure 1d. (a) Top view. (b) Side view (along the armchair direction). Dashed lines define the $2\sqrt{3} \times \sqrt{3}$ supercell. Note that all the −OH form H bonds with neighboring −OH or −O−, and both −O− groups are distributed evenly on both sides of the graphene sheet. The Ti sites are *Z*2.5, *Z*2.5′, or *A*3, where *Z* stands for *zigzag* and *A* stands for *armchair*, and the number indicates the separation between O atoms (in units of C−C bonds along the carbon chain). Due to the high O packing density, each Ti always binds to two O.

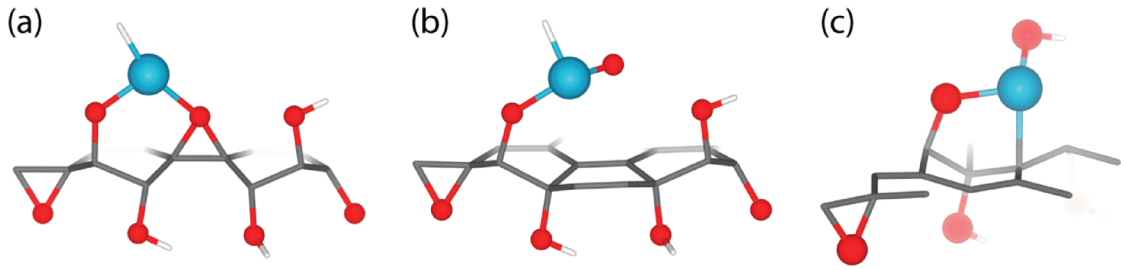

Figure 3. Ti reaction pathway at the *Z*2.5 site. (a) Initial structure, where the H atom (of the −OH group) on the far-left top-layer oxygen atom has migrated to the Ti atom, (b) the uplift of the epoxy oxygen, and (c) the direct binding of the Ti to carbon atoms.

ing between two −OH lowers the energy by 28 kJ/mol. The corresponding OH···O distance is 1.88 Å. These values are similar to those calculated for a water dimer (22 kJ/mol and 1.91 Å, respectively) at the same theoretical level. Condition ii suggests that the −O− and −OH should be evenly distributed on both sides of the graphene sheet. Taking again the example in Figure 1d, if we flip the −O− from one side to another, indeed the total energy would increase by 27 kJ/mol. A careful examination shows that condition iii can only be fulfilled by sites 1, 3, and 5. As it turns out, site 5 is higher in energy than site 1 by 62 kJ/mol. Condition iv is fulfilled by sites 1, 2, and 3, which are in the same hexagonal carbon ring. Among all the considered sites in Figure 1c, site 1 and site 3 have the lowest-energy and are almost the same in energy.

Thus, these two motifs are exceptionally stable and should be abundant on GO at least when the oxygen group coverage is low or modest. In this paper, we will use one of them, as shown in Figure 1d, as a representative to construct an extended GO structure. The smallest cell with the 1:1:1 carbon ratios would be a $\sqrt{3} \times \sqrt{3}$ cell containing six C atoms (or one motif unit). When repeating this surface cell, however, all of the epoxies would have to be on the same side of the graphene sheet. Similarly, all the hydroxyls would have to be on the other side. This turns out to be energetically unfavorable. To avoid such a situation, we double the cell size to $2\sqrt{3} \times \sqrt{3}$ (see Figure 2). Note that in Figure 1d there is on average only half hydrogen bond per −OH. By doubling the cell, each hydroxyl can form a hydrogen bond either with another hydroxyl or with an epoxy. Thus, there exists now one hydrogen bond per −OH. The doubling of the cell lowers the system energy by 170 kJ/mol-C_{12} (or per $2\sqrt{3} \times \sqrt{3}$ cell). About 60 kJ/mol-C_{12} can be accounted for by the two extra hydrogen bonds to the epoxies. The remaining 110 kJ/mol-C_{12} comes from the long-range even distribution of the O groups on both sides of the graphene sheet. Its physical origin is presumably also the reduction of strain energy and Coulomb repulsion.

Ti Anchoring on GO. The binding energy of Ti is defined by

$$E_b(\mathrm{Ti}) = E(\mathrm{GO}) + E(\mathrm{Ti}) - E(\mathrm{Ti/GO})$$

where E(GO), E(Ti), and E(Ti/GO) are the total energy of GO, Ti atom, and Ti on GO, respectively. On the GO surface, there are three possible Ti sites labeled *Z*2.5, *Z*2.5′, and *A*3 (see Figure 2a and its caption). In all three cases, the Ti, upon bonding to an O, will form another bond with a second neighboring O. As a result, the Ti always straddles in a bridge site between two O. This is because the relatively high O density.

GO is different from mesoporous silica. It possesses reactive epoxy oxygen, as well as open sp^2 carbon. These differences may result in Ti reactions with GO that are not present on mesoporous silica surface. Indeed, we find that, when the Ti is on either the *Z*2.5 or *Z*2.5′ site, the epoxy is detached from the graphene. Figure 3 shows what happens at *Z*2.5 in three frames. Initially, the Ti is anchored onto one −O− and one −OH (frame a). It lifts up the epoxy oxygen (frame b), which allows the Ti to bind directly to the C atoms underneath (frame c). The entire process is barrierless, and the final structure is more stable by 2 eV.

For hydrogen-storage purpose, such a Ti-epoxy reaction may not be desirable. As storage takes place in a relatively H-abundant environment, we may eliminate this reaction by hydrogenating the epoxy, which at the

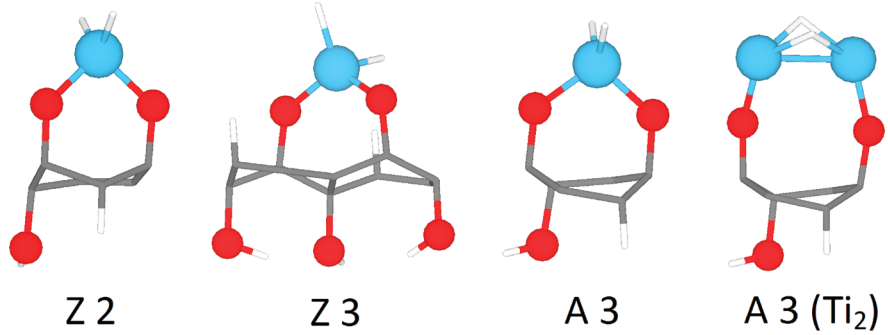

Figure 4. Stable Ti/GO motifs at three possible Ti sites in Figure 2a. Due to the hydrogenation of epoxy, however, the O−O distance, and hence the numerical labeling, has changed. A Ti dimerized motif at *A*3 site is also shown.

TABLE 1. Anchoring O−O Separation (in Å), Ti Binding Energy (in kJ/mol-Ti), Sequential H_2 Binding Energies (in kJ/mol-H_2), and H−H Bond Length (in Å) on Hydrogenated GO (* Indicates Dissociated H_2 That Should Not Be Considered for Reversible Hydrogen Storage); For Comparison, LDA Results for Ti at the *Z*2 Site Are Also Given

		Ti	1st H_2		2nd H_2		3rd H_2		4th H_2	
site	d_{O-O}	E_b	E_b	d_{H-H}	E_b	d_{H-H}	E_b	d_{H-H}	E_b	d_{H-H}
*Z*2	2.63	481	30	0.82	18	0.78	—	—	—	—
(LDA)	(2.58)	(510)	(65)	(0.87)	(33)	(0.82)				
*Z*3	3.16	445	25	0.85	15	0.78	—	—	—	—
*A*3	2.83	475	29	0.83	18	0.78	—	—	—	—
*A*3 (Ti_2)	3.19	427	96*	—	41	0.79	22	0.80	14	0.79
*Z*4	5.10	291	93*	—	28	0.86	36	0.81	24	0.85

same time may also eliminate sp^2 carbon. Hydrogenation of sp^2 graphene into full sp^3 graphane has been experimentally demonstrated recently.[26] Our computations show that the hydrogenation of epoxy by H_2 not only converts it to a hydroxyl but also simultaneously converts an sp^2 carbon to sp^3 carbon. This is energetically more favorable by 0.2 eV per H over the hydrogenation of graphene.

Similar to the untreated GO, there are three Ti anchoring sites on hydrogenated GO (HGO): they are labeled as *Z*2, *Z*3, and *A*3 in Figure 4. Due to the hydrogenation, the *Z*2.5 and *Z*2.5′ sites in Figure 2a become the *Z*3 and *Z*2 sites, respectively. Table 1 summarizes the results. Ti@*Z*2 has a binding energy of 481 kJ/mol-Ti and is most stable. The anchoring O−O separation is 2.63 Å. Ti@*A*3 has a binding energy of 475 kJ/mol-Ti, and the O−O separation is 2.83 Å. Ti@*Z*3 has a binding energy of 445 kJ/mol-Ti, and the O−O separation is 3.16 Å. The Ti binding energy is thus correlated with the O−O separation. These energies are comparable to those for Ti on mesoporous silica and can be compared to Ti_2 dimer in vacuum (278 kJ/mol). The similarity with mesoporous silica suggests that Ti will not leave GO to form any clusters. To further confirm the Ti stability, we perform vibrational analysis to verify that none of the Ti motifs has any structural instability associated with imaginary frequencies. Figure 4 also shows a surface Ti dimer, Ti_2@*A*3. The calculated binding energy for this on-site dimer is 427 kJ/mol-Ti, which is 108, 96, and 36 kJ/mol-Ti_2 smaller than those for Ti@*Z*2, *A*3, and *Z*3, respectively. Therefore, inserting Ti onto already existing Ti sites, which could serve as the first step of onsite clustering, is also energetically unfavorable.

Hydrogen-Storage Properties. Sequential H_2 binding energy to Ti (anchored on HGO) is defined as

$$E_b = E[\mathrm{Ti/HGO(H_2)}_{n-1}] + E(\mathrm{H_2}) - E[\mathrm{Ti/HGO(H_2)}_n]$$

where $E[\mathrm{Ti/HGO(H_2)}_n]$ and $E(H_2)$ are the total energies of Ti/HGO with *n* adsorbed H_2 and isolated H_2, respectively. Ti@*Z*2 (Figure 5a) can take two H_2: the first at 30 kJ/mol-H_2 and the second at 18 kJ/mol-H_2.[27] The corresponding Ti−H_2 distances are 1.9 and 2.1 Å, respectively. H_2 binding to Ti@*Z*3 (Figure 5b) and *A*3 (Figure 5c) is essentially the same as that to Ti@*Z*2. For Ti_2@*A*3 (Figure 5d), the first H_2 dissociates to form dihydride with a formation energy of 96 kJ/mol-H_2. Subsequent H_2 adsorption, however, resumes the molecular form. For the second, third, and fourth H_2, the sequential binding energies are 41, 22, and 14 kJ/mol-H_2, respectively. The distances between the H_2 molecules and Ti are all within 2.1 Å. The results for hydrogen binding are also given in Table 1. It shows that the H−H bond length is significantly longer than that calculated for free H_2 molecule (0.75 Å). The facts that the adsorbed H_2 takes the side-on configuration and the binding energies in Table 1 can be as large as 41 kJ/mol suggest that the Ti−H_2 binding is of Kubas-type.[3,28]

To use GO for hydrogen storage, it is necessary to consider how accessible are the surface areas when the GO layers are stacked together. Interestingly, open GO structures can be relatively easily fabricated. In a recent patent application disclosure,[29] thermally exfoliated GO bulk materials have been experimentally prepared. The measured surface areas range from 300 to 2500 m^2/g. We can estimate what would be the surface area required for hydrogen storage. On the basis of the GO structure discussed above, we obtain a surface area of 1654 m^2/g. Thus, there are enough surface areas for hydrogen storage in such GO materials.

To increase H capacity, one needs to optimize Ti separation. A recent paper[30] revealed that a 2 × 2 graphene cell yields the optimal calcium separation for hydrogen storage. The atomic radii of Ca and Ti are 2.23 and 2.00 Å, respectively. Neglecting the small size difference, we arrive at the *Z*4 structure in Figure 6 for Ti.

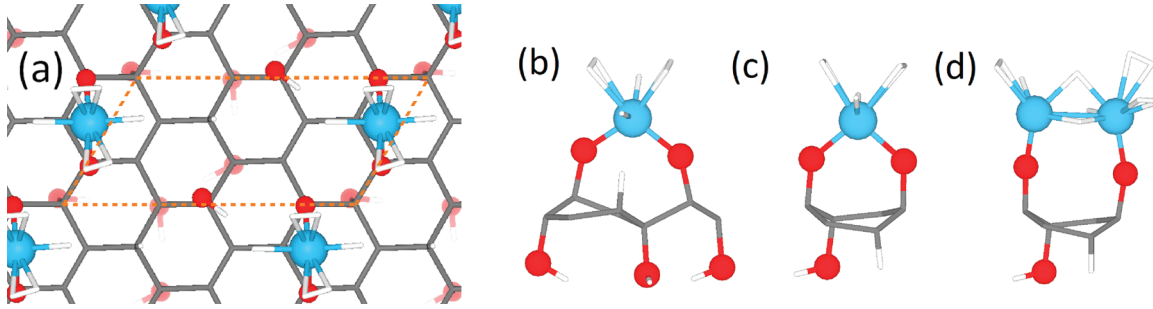

Figure 5. (a) Top view: H_2 binding to Ti@*Z*2. (b−d) Side views: H_2 binding to Ti@*Z*3, *A*3, and Ti_2@*A*3, respectively.

Here, the pairing of −OH on the opposite sides stabilizes the system. The O−O separation on the same side is 5.1 Å, and the O/C ratio is 1:4. This coverage is close to a recent experimental report[15] for epoxy on graphene with an O/C ratio of 1:5. Thus, one would only have to hydrogenate the GO without the removal of O to test our theory. The calculated binding energy for Ti (291 kJ/mol-Ti) is smaller than Ti with two O anchors but is still larger than that of Ti dimer in vacuum.

Table 1 shows the results for H_2 binding. Each Ti can take four H_2 but the first dissociates with a Ti−H binding energy of 93 kJ/mol-H_2. The rest of the H_2 do not dissociate. Interestingly, when the fourth H_2 is adsorbed, the first dissociated H_2 also reverses back to its original molecular form. The average binding energy for the last three H_2 is 29 kJ/mol-H_2. Following Lee *et al.*,[31] we estimated the upper bound on the gravimetric H density at standard conditions to be 4.9 wt %. Note that the dihydride is too strongly bounded and is not considered in our estimation. To find the optimal volumetric density, we calculated the interlayer distances for Ti−HGO sheets with fully loaded H_2 by both generalized gradient approximation (GGA) and local density approximation (LDA). The distances are 14 Å from GGA, corresponding to a volumetric density of 64 g/L, and 12 Å from LDA, corresponding to a volumetric density of 74 g/L. GGA tends to overestimate, whereas LDA tends to underestimate, the interlayer distance. Thus the real volumetric density could be between 64 and 74 g/L.

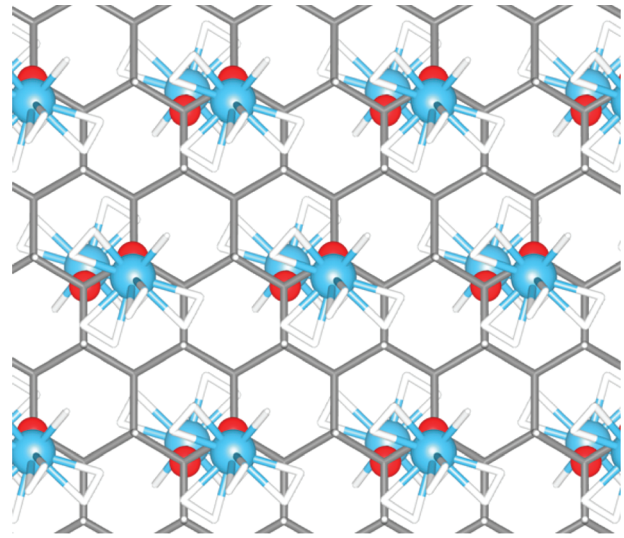

Figure 6. *Z*4 structure on HGO fully loaded with H_2. It has a 2 × 2 Ti periodicity, and the O−O separation on the same side is d_{O-O} = 5.1 Å.

CONCLUSIONS

In summary, we have investigated the structural properties of GO and the feasibility of using GO to anchor Ti for hydrogen storage by means of first-principles computations. We propose that on GO there exist stable structural motifs as the basic function units of oxygen groups. GO could be an excellent substrate for Ti, but for hydrogen storage, it requires the hydrogenation of epoxy and open sp^2 sites. On hydrogenated GO, the Ti binding is strong, comparable to that on Ti-grafted mesoporous silica, and enough to prevent Ti clustering. Dihydrogen binding energy is also favorable for room-temperature storage. In view of the recent success of enhanced multi-H_2 binding on Ti-grafted mesoporous silica and the well-established methods for synthesis of supported catalysts from organometallic precursor molecules, Ti-anchored GO may offer a feasible solution for hydrogen storage.

METHODS

The computations are based on the density functional theory (DFT) in the Perdew−Burke−Ernzerhof[32] generalized gradient approximation or in the local density approximation.[33,34] Frozen-core all-electron projector augmented wave (PAW) method,[35] as implemented in the VASP code,[36] is used. The cutoff energy for the plane-wave basis expansion is 500 eV. We employ the first-order Methfessel−Paxton partial occupation scheme[37] with a 10 meV smearing. A two-dimensional periodic supercell is used with adjacent GO layers separated by a 20 Å thick vacuum region. For the Brillouin zone integration, a 3 × 6 **k**-point grid is used for a $2\sqrt{3} \times \sqrt{3}$ cell, which is equivalent to a 10 × 10 grid for the 1 × 1 primitive cell. Both atomic positions and lattice parameters are fully relaxed until the forces on all the atoms are less than 0.01 eV · Å^{-1}. For the analysis of vibrational modes, we use finite-difference method with a displacement of 0.015 Å.

Acknowledgment. The authors thank the Computational Center for Nanotechnology Innovations (CCNI) at RPI for their supercomputer facilities. This work was supported by DOE/OS/BES and DOE/EERE under Contract No. DE-AC36-08GO28308 and subcontracts to RPI No. J30546/J90336, DOE BES/CMSN Program, NSF Grant CHE-0716718, and the Institute for Functional Nanomaterials (NSF Grant 0701525), the Program for New Century Excellent Talents in University of China (NCET06-0281), and the National Natural Science Foundation of China (No. 10774019).

REFERENCES AND NOTES

1. Bhatia, S. K.; Myers, A. L. Optimum Conditions for Adsorptive Storage. *Langmuir* **2006**, *22*, 1688–1700.
2. Lochan, R. C.; Head-Gordon, M. Computational Studies of Molecular Hydrogen Binding Affinities: The Role of Dispersion Forces, Electrostatics, and Orbital Interactions. *Phys. Chem. Chem. Phys.* **2006**, *8*, 1357–1370.
3. Zhao, Y.; Kim, Y.-H.; Dillon, A. C.; Heben, M. J.; Zhang, S. B. Hydrogen Storage in Novel Organometallic Buckyballs. *Phys. Rev. Lett.* **2005**, *94*, 155504-1–155504-4.
4. Yildirim, T.; Ciraci, S. Titanium-Decorated Carbon Nanotubes as a Potential High-Capacity Hydrogen Storage Medium. *Phys. Rev. Lett.* **2005**, *94*, 175501-1–175501-4.
5. Forster, P. M.; Eckert, J.; Heiken, B. D.; Parise, J. B.; Yoon, J. W.; Jhung, S. H.; Chang, J. S.; Cheetham, A. K. Adsorption of Molecular Hydrogen on Coordinatively Unsaturated Ni(II) Sites in a Nanoporous Hybrid Material. *J. Am. Chem. Soc.* **2006**, *128*, 16846–16850.
6. Ma, S. Q.; Zhou, H. C. A Metal−Organic Framework with Entatic Metal Centers Exhibiting High Gas Adsorption Affinity. *J. Am. Chem. Soc.* **2006**, *128*, 11734–11735.

7. Dinca, M.; Dailly, A.; Liu, Y.; Brown, C. M.; Neumann, D. A.; Long, J. R. Hydrogen Storage in a Microporous Metal−Organic Framework with Exposed Mn^{2+} Coordination Sites. *J. Am. Chem. Soc.* **2006**, *128*, 16876–16883.
8. Vitillo, J. G.; Regli, L.; Chavan, S.; Ricchiardi, G.; Spoto, G.; Dietzel, P. D. C.; Bordiga, S.; Zecchina, A. Role of Exposed Metal Sites in Hydrogen Storage in MOFs. *J. Am. Chem. Soc.* **2008**, *130*, 8386–8396.
9. Hamaed, A.; Trudeau, M.; Antonelli, D. M. H_2 Storage Materials (22 kJ/mol) Using Organometallic Ti Fragments as σ-H_2 Binding Sites. *J. Am. Chem. Soc.* **2008**, *130*, 6992–6999.
10. Sun, Q.; Wang, Q.; Jena, P.; Kawazoe, Y. Clustering of Ti on a C_{60} Surface and Its Effect on Hydrogen Storage. *J. Am. Chem. Soc.* **2005**, *127*, 14582–14583.
11. Lee, H.; Nguyen, M. C.; Ihm, J. Titanium-Functional Group Complexes for High-Capacity Hydrogen Storage Materials. *Solid State Commun.* **2008**, *146*, 431–434.
12. Shevlin, S. A.; Guo, Z. X. High-Capacity Room-Temperature Hydrogen Storage in Carbon Nanotubes *via* Defect-Modulated Titanium Doping. *J. Phys. Chem. C* **2008**, *112*, 17456–17464.
13. Kim, G.; Jhi, S.-H. Effective Metal Dispersion in Pyridinelike Nitrogen Doped Graphenes for Hydrogen Storage. *Appl. Phys. Lett.* **2008**, *92*, 013106-1–013106-3.
14. Meng, S.; Kaxiras, E.; Zhang, Z. Y. Metal-Diboride Nanotubes as High-Capacity Hydrogen Storage Media. *Nano Lett.* **2007**, *7*, 663–667.
15. Zhang, C. G.; Zhang, R. W.; Wang, Z. X.; Zhou, Z.; Zhang, S. B.; Chen, Z. Ti-Substituted Boranes as Hydrogen Storage Materials: A Computational Quest for Ideal Combination of Stable Electronic Structure and Optimal Hydrogen Uptake. *Chem.—Eur. J.* **2009**, *15*, 5910–5919.
16. Jung, I.; Dikin, D. A.; Piner, R. D.; Ruoff, R. S. Tunable Electrical Conductivity of Individual Graphene Oxide Sheets Reduced at "Low" Temperatures. *Nano Lett.* **2008**, *8*, 4283–4287.
17. Mkhoyan, K. A.; Contryman, A. W.; Silcox, J.; Stewart, D. A.; Eda, G.; Mattevi, C.; Miller, S.; Chhowalla, M. Atomic and Electronic Structure of Graphene-Oxide. *Nano Lett.* **2009**, *9*, 1058–1063.
18. Park, S.; Lee, K.-S.; Bozoklu, G.; Cai, W.; Nguyen, S. T.; Ruoff, R. S. Graphene Oxide Papers Modified by Divalent Ions-Enhancing Mechanical Properties via Chemical Cross-Linking. *ACS Nano* **2008**, *2*, 572–578.
19. Chattopadhyay, J.; Mukherjee, A.; Hamilton, C. E.; Kang, J.; Chakraborty, S.; Guo, W.; Kelly, K. F.; Barron, A. R.; Billups, W. E. Graphite Epoxide. *J. Am. Chem. Soc.* **2008**, *130*, 5414–5415.
20. Talyzin, A. V.; Solozhenko, V. L.; Kurakevych, O. O.; Szabó, T.; Dékány, I.; Kurnosov, A.; Dmitriev, V. Colossal Pressure-Induced Lattice Expansion of Graphite Oxide in the Presence of Water. *Angew. Chem., Int. Ed.* **2008**, *47*, 8268–8271.
21. Kudin, K. N.; Ozbas, B.; Schniepp, H. C.; Prud'homme, R. K.; Aksay, I. A.; Car, R. Raman Spectra of Graphite Oxide and Functionalized Graphene Sheets. *Nano Lett.* **2008**, *8*, 36–41.
22. Paci, J. T.; Belytschko, T.; Schatz, G. C. Computational Studies of the Structure, Behavior upon Heating, and Mechanical Properties of Graphite Oxide. *J. Phys. Chem. C* **2007**, *111*, 18099–18111.
23. He, H. Y.; Klinowski, J.; Forster, M.; Lerf, A. A New Structural Model for Graphite Oxide. *Chem. Phys. Lett.* **1998**, *287*, 53–56.
24. Boukhvalov, D. W.; Katsnelson, M. I. Modeling of Graphite Oxide. *J. Am. Chem. Soc.* **2008**, *130*, 10697–10701.
25. Cai, W. W.; Piner, R. D.; Stadermann, F. J.; Park, S.; Shaibat, M. A.; Ishii, Y.; Yang, D.; Velamakanni, A.; An, S. J.; Stoller, M.; An, J.; Chen, D.; Ruoff, R. S. Synthesis and Solid-State NMR Structural Characterization of 13C-Labeled Graphite Oxide. *Science* **2008**, *321*, 1815–1817.
26. Elias, D. C.; Nair, R. R.; Mohiuddin, T. M. G.; Morozov, S. V.; Blake, P.; Halsall, M. P.; Ferrari, A. C.; Boukhvalov, D. W.; Katsnelson, M. I.; Geim, A. K.; Novoselov, K. S. Control of Graphene's Properties by Reversible Hydrogenation: Evidence for Graphane. *Science* **2009**, *323*, 610–613.
27. It has been suggested that GGA gives a lower limit, while LDA gives an upper limit, to the H_2 binding energy: Gao, Y.; Zeng, X. C. *Ab Initio* Study of Hydrogen Adsorption on Benzenoid Linkers in Metal−Organic Framework Materials. *J. Phys.: Condens. Matter* **2007**, *19*, 386220-1–386220-8. We performed LDA calculations for Ti at the *Z*2 site. The binding energies for the first and second adsorbed H_2 are 65 and 33 kJ/mol-H_2, respectively (see Table 1), in line with the prediction.
28. Kubas, G. J. Fundamentals of H_2 Binding and Reactivity on Transition Metals Underlying Hydrogenase Function and H_2 Production and Storage. *Chem. Rev.* **2007**, *107*, 4152–4205.
29. Prud'homme, R. K.; Aksay, I. A.; Adamson, D.; Abdala, A. United States Patent Application 20090054272.
30. Kim, Y. H.; Sun, Y. Y.; Zhang, S. B. Ab Initio Calculations Predicting the Existence of an Oxidized Calcium Dihydrogen Complex to Store Molecular Hydrogen in Densities up to 100 g/L. *Phys. Rev. B* **2009**, *79*, 115424-1–115424-5.
31. Lee, H.; Choi, W. I.; Ihm, J. Combinatorial Search for Optimal Hydrogen-Storage Nanomaterials Based on Polymers. *Phys. Rev. Lett.* **2006**, *97*, 056104-1–056104-4.
32. Perdew, J. P.; Burke, K.; Ernzerhof, M. Generalized Gradient Approximation Made Simple. *Phys. Rev. Lett.* **1996**, *77*, 3865–3868.
33. Ceperley, D. M.; Alder, B. J. Ground State of the Electron Gas by a Stochastic Method. *Phys. Rev. Lett.* **1980**, *45*, 566–569.
34. Perdew, J. P.; Zunger, A. Self-Interaction Correction to Density-Functional Approximations for Many-Electron Systems. *Phys. Rev. B* **1981**, *23*, 5048–5079.
35. Blöchl, P. E. Projector Augmented-Wave Method. *Phys. Rev. B* **1994**, *50*, 17953–17979.
36. Kresse, G. Furthmüller, Efficient Iterative Schemes for *Ab Initio* Total-Energy Calculations Using a Plane-Wave Basis Set. *Phys. Rev. B* **1996**, *54*, 11169–11186.
37. Methfessel, M.; Paxton, A. T. High-Precision Sampling for Brillouin-Zone Integration in Metals. *Phys. Rev. B* **1989**, *40*, 3616–3621.